08

Electrophysical properties of hybrid graphene-nanotube quasi-2D structures

© M.M. Slepchenkov[1], P.V. Barkov[1], O.E. Glukhova[1,2]

[1] Saratov National Research State University,
Saratov, Russia
[2] I.M. Sechenov First Moscow State Medical University,
Moscow, Russia

E-mail: slepchenkovm@mail.ru

Received April 30, 2025
Revised September 8, 2025
Accepted November 11, 2025

The paper presents the results of a study of the influence of structural features on the electrophysical properties of hybrid thin-film graphene-nanotube structures. The object of the study is quasi-2D films formed by two-layer graphene and chiral single-walled carbon nanotubes (SWCNTs) of sub- and nanometer diameters. The chirality indices and the diameter of the nanotube, the type of stacking of graphene layers, the mutual arrangement of nanotubes and graphene in the graphene-SWCNT hybrid are considered as structural features. The electrophysical properties are estimated by the calculated values of electrical conductivity and by the volt-ampere characteristics.

Keywords: graphene-nanotube hybrids, quantum electron transport, transmission fucntion, volt-ampere characteristics.

DOI: 10.61011/PSS.2025.12.63107.8104k-25

1. Introduction

Carbon nanomaterials are the subject of many theoretical and experimental studies due to the wide variety of allotropic forms of carbon, which determines the rich range of their properties [1]. Graphene and nanotubes are currently attracting the attention of researchers and developers among allotropic carbon modifications [2]. Combining graphene and carbon nanotubes (CNTs) into a hybrid structure has stimulated the emergence of a new class of carbon nanomaterials endowed with promising properties [3–6]. The synergistic effect of the integration of two-dimensional graphene and one-dimensional nanotubes makes it possible to improve the mechanical, electrochemical, electrical and optical properties of graphene-nanotube hybrids compared with isolated carbon components [7–10]. In this regard, hybrid carbon structures are used in various electronic, optoelectronic and energy storage devices such as supercapacitors, logic inverters, optoelectronic memory, photodetectors, electroluminescent light emitters [11,12].

There are three topological types of graphene-CNT hybrid structure [10]: 1) CNTs placed horizontally with respect to the graphene plane; 2) CNTs placed vertically with respect to the graphene plane; 3) CNTs wrapped with graphene. The first two topological types are more common than the third and are the object of research in many scientific articles [4,5]. Modern technologies for the synthesis of graphene and CNTs make it possible to obtain nanotubes of various chirality and diameter, graphene in the form of a monolayer and layered structure with various types of layering, as well as to implement different variants of the mutual arrangement of graphene and CNT in a hybrid and methods of their connection [4,5,11]. Therefore, we can talk about a potential geometric and topological variety of structural configurations of graphene-nanotube hybrids. In this regard, an important role is assigned to research performed by atomistic modeling methods, which make it possible to predict which types of structural configurations of the graphene-CNT hybrid demonstrate the most advantageous physico-chemical properties. When designing electronic nanodevices based on graphene-nanotube hybrids, it is important to understand the role of the features of their atomic structure in the transport of electrons through the device. Various research groups are working on solving this issue using atomic modeling methods [12–14]. The studied objects in published papers are graphene-nanotube hybrids with armchair or zigzag nanotubes and with single-layer graphene. At the same time, a number of key structural features of synthesized graphene and nanotubes were not taken into account by the authors when constructing atomistic models of graphene-nanotube structures. In particular, most of the SWCNT obtained during synthesis are chiral tubes with a diameter of $0.7-1.3$ nm. It has also been experimentally shown that bilayer graphene is characterized by higher stability compared to monolayer [15]. The object of research in this paper is quasi-2D films formed by bilayer graphene and chiral SWCNT of sub- and nanometer diameters. The purpose of this study is to identify patterns of the influence of structural features on the electrophysical properties of hybrid thin-film structures bilayer graphene-SWCNT. Structural features include the chirality indices and the diameter of a nanotube, the type of graphene layers

laid, and the relative position of nanotubes and graphene in a hybrid.

2. Calculation method

The calculations were performed using the self-consistent charge density-functional tight-binding (SCC-DFTB) method [16], implemented in the DFTB+ software package [17]. The Van der Waals character of the interaction between bilayer graphene and a nanotube in the super cell of a graphene-nanotube hybrid was taken into account in the framework of the Lennard-Jones dispersion correction scheme [18]. The electrical conductivity of the studied structures was calculated within the framework of the Landauer-Buttiker [19] formalism using a formula of the form

$$G = 2e^2/h \int_{-\infty}^{\infty} T(E)F_T(E - E_F)dE, \qquad (1)$$

where $T(E)$ is the average electron transmission function, E_F is the Fermi level of the electrodes, e^2/h is the conduction quantum, F_T is the thermal broadening function energy levels, defined as

$$F_T = \frac{1}{4k_B T}\mathrm{sech}^2\left(\frac{E - E_F}{2k_B T}\right), \qquad (2)$$

where k_B is the Boltzmann constant, T is the temperature.

The electron transmission function $T(E)$ is defined by an expression of the form

$$T(E) = \mathrm{Tr}\left(\Gamma_S(E)G_C^A(E)\Gamma_D(E)G_C^R(E)\right), \qquad (3)$$

where $G_C^A(E)$ and $G_C^R(E)$ are the leading and lagging Green matrices describing the interaction of the simulated system with the electrodes, and $\Gamma_S(E)$ and $\Gamma_D(E)$ are the broadening matrices of the energy levels of the source electrodes and the drain. Calculations of the electrical conductivity characteristics were performed at a temperature of 300 K.

3. Selected configurations

The studies were carried out for two structural configurations of a graphene-nanotube film formed by bilayer graphene with an alternating layer order of AB and chiral SWCNT. Figure 1 shows the super-cells of the configurations under consideration, obtained as a result of optimization of the atomic structure, which was carried out by achieving a global minimum of total energy. The first configuration (model V1) is formed by bilayer graphene with a shear value of the upper layer relative to the lower one ~ 0.1 nm and a metal SWCNT (12,6) diameter ~ 1.2 nm (Figure 1, *a*). The second configuration (model V2) is formed by bilayer graphene with a displacement of the upper layer relative to the lower one ~ 0.3 nm and a semiconductor SWCNT (8,4) diameter ~ 0.8 nm (Figure 1, *b*). The selected nanotubes (12,6) and (8,4) are among the most frequently synthesized SWCNT with high purity (more than 90 %) [20]. In addition, nanotubes of different types of conductivity have been selected to show how the type of conductivity of SWCNT affects the electrophysical properties of a hybrid graphene-nanotube film. In both configurations, the graphene bilayer was located above the SWCNT, however, in the case of the V2 model, the graphene layers were located at an angle to the surface of the nanotube. It should be emphasized that such an inclined arrangement of the layers is the result of optimizing the geometric parameters of the super-cell. The equilibrium distance between bilayer graphene and SWCNT is 0.33 nm for the V1 and 0.28 nm for the V2 model, whereas between graphene layers — 0.36 nm for V1 and 0.32 nm for V2. It can also be seen from Figure 1 that during the formation of the hybrid carbon structure, fragments of bilayer graphene and SWCNT were deformed. The degree of deformation of the nanotube, estimated by the ratio between the radii in the direction of the axes X and Z, was 1.2 for the V1 model and 1.1 for the V2 model. The constructed super cells were tested for thermodynamic stability, which was estimated by the value of the binding energy E_b. For the super cell model V1 E_b is ~ -0.14 eV/atom, for the super cell model V2 E_b is ~ -0.18 eV/atom. Negative values of the binding energy indicate that the studied structures are stable in energy.

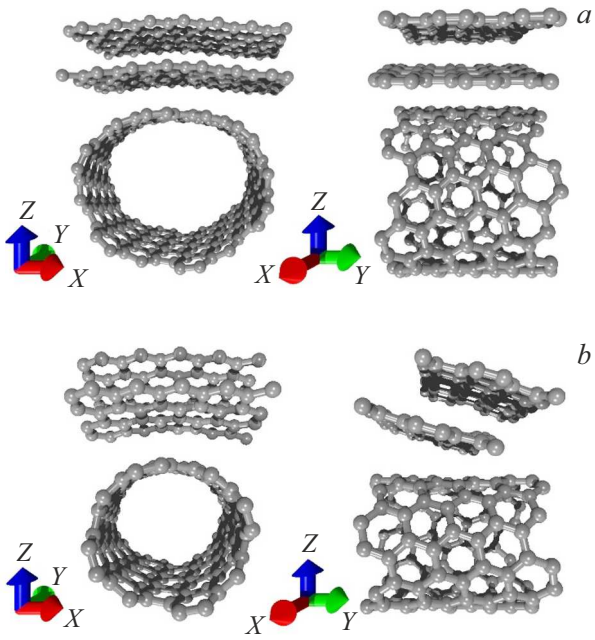

Figure 1. Super-cells of quasi-2D films: *a* — bilayer graphene-SWCNT (12,6) and *b* — bilayer graphene-SWCNT (8,4).

Figure 2 shows expanded fragments of graphene-nanotube films obtained as a result of super-cell translation along the axes X and Y. It is clearly seen that in the V2 model graphene is represented as layers of finite width (3 hexagon) in the armchair direction (axis Y), but

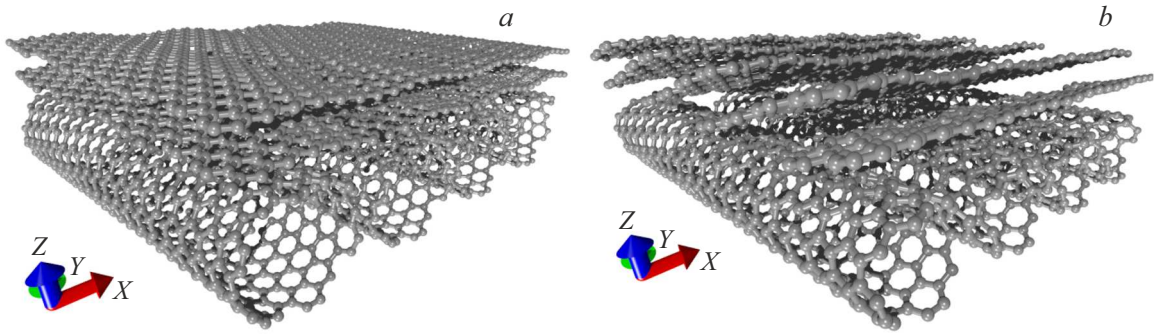

Figure 2. Expanded fragments of quasi-2D films: *a* — bilayer graphene-SWCNT (12,6) and *b* — bilayer graphene-SWCNT (8,4), obtained as a result of super-cell translation along the axes *X* and *Y*.

infinitely extended in the zigzag direction (axis *X*) of a hexagonal lattice similar to graphene nanoribbons of the zigzag type. In the V1 model, graphene has infinitely extended layers in the zigzag and armchair directions.

4. Results and discussion

Figure 3 shows the volt-ampere characteristics (VAC) for models V1 and V2 of graphene-nanotube films calculated during current transfer along nanotubes. It can be seen from the figure that the V1 model is characterized by large current values compared to the V2 model at the same voltage values. The greatest difference in current values between the models is observed in the voltage range up to 1 V. In particular, it reaches 50 times at a voltage of 0.4 V and 70 times at a voltage of 0.6 V. The electrical conductivity G is 43.4 μS for the V1 model and 3.8 μS for the V2 model. To analyze the results obtained, graphs of the transmission function $T(E)$ were constructed for each of the models, which characterizes the probability of electrons passing through a potential barrier (Figure 4). In addition to images of the functions $T(E)$ of graphene-nanotube films, the graphs also depict the functions of $T(E)$ bilayer graphene fragments and nanotubes that are part of the super-cells of the structural configurations under consideration. Figure 4, *a* shows that the profile of the function $T(E)$ of the bilayer graphene-SWCNT film (12,6) repeats the contours of the profile $T(E)$ of bilayer graphene, however, the graph itself is shifted along the ordinate axis by 2 units due to the influence of a metal nanotube (12,6), which has a constant function $T(E)$ equal to two in the energy range under consideration near the Fermi level (-4.68 eV). In the case of a bilayer graphene-SWCNT film (8,4) (Figure 4, *b*), the profile $T(E)$ near the Fermi level (-4.86 eV) completely repeats the profile $T(E)$ of a semiconductor nanotube (8,4), which is characterized by the presence of a transport gap, the size of which (0.7 eV) completely coincides with the size of the transport gap of the graphene-SWCNT film (8,4). The contribution of bilayer graphene is not significant in this case, since, as noted above, the super cell of the V2 model includes fragments of graphene in the form of zigzag nanoribbons conducting current in the zigzag direction (perpendicular to the nanotubes) of the hexagonal lattice.

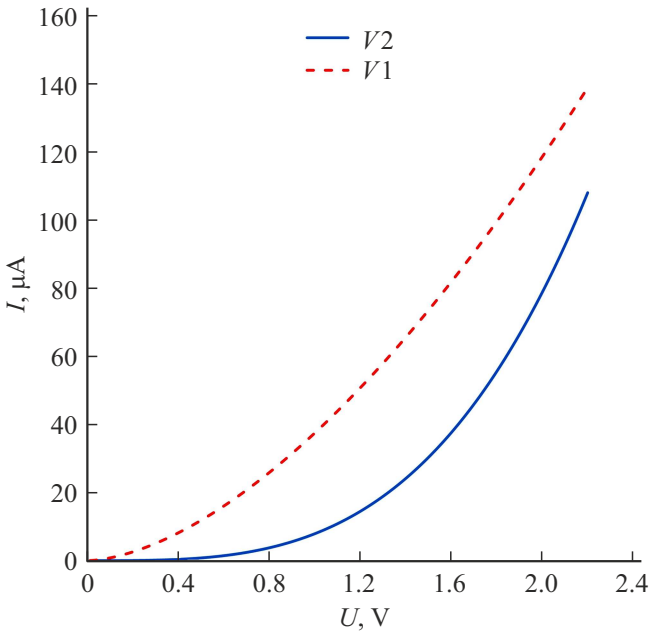

Figure 3. Volt-ampere characteristics of quasi-2D films bilayer graphene-SWCNT (12,6) (model V1) and bilayer graphene-SWCNT (8,4) (model V2) during current transfer along nanotubes (axis *Y*).

5. Conclusion

Thus, along with the conductive properties of bilayer graphene and SWCNT, determined by their structural features (the type of stacking layers in bilayer graphene and the amount of shear between the layers, the type of conductivity and the diameter of the SWCNT), the relative position of bilayer graphene and nanotubes in the hybrid architecture plays an important role in shaping the electrophysical properties of graphene-nanotube films. The

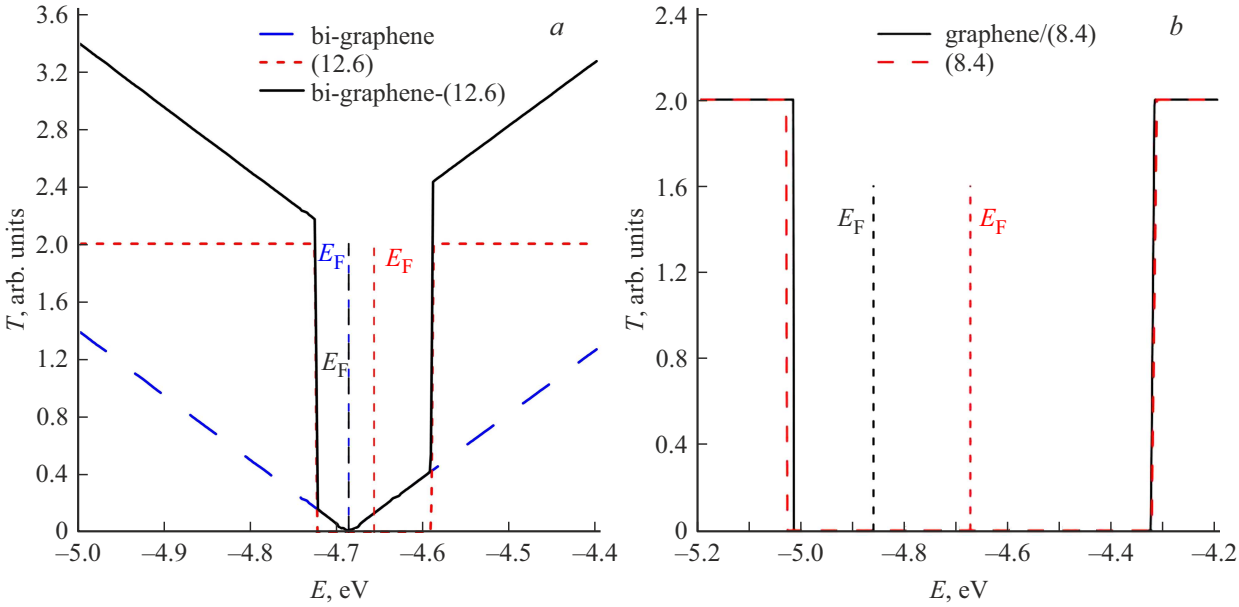

Figure 4. Graphs of the electron transmission function $T(E)$ of quasi-2D films: *a* — bilayer graphene-SWCNT (12,6); *b* — bilayer graphene-SWCNT (8,4), as well as fragments of bilayer graphene and nanotubes, which are part of their super-cells. The vertical dotted lines show the Fermi levels of graphene-SWCNT films (black), bilayer graphene (blue), and nanotubes (red).

inclined arrangement of graphene sheets with respect to the surface of the SWCNT (8,4), achieved with a shift between graphene layers ~ 0.3 nm in the super cell bilayer graphene SWCNT (8,4), as well as the semiconductor type of conductivity SWCNT (8,4) caused a lower current value models V2 (50 times at 0.4 V, 6 times at 0.8 V, 2.5 times at 1 V) compared to the V1 model. The revealed patterns of topological control of electrical conductivity open up new possibilities in the design of nanoelectronic devices based on hybrid carbon films. In particular, such films can be used in nanotransistors and in nanoscale logic gates. By appropriately selecting the structural features of graphene-nanotube hybrid films, it is possible to control the current characteristics of devices based on them.

Funding

This work was supported by a grant from the Russian Science Foundation (project No. 24-79-10316, https://rscf.ru/project/24-79-10316/).

Conflict of interest

The authors declare no conflict of interest.

References

[1] O.S. Ayanda, A.O. Mmuoegbulam, O. Okezie, N.I. Durumin Iya, S.E. Mohammed, P.H. James, A.B. Muhammad, A.A. Unimke, S.A. Alim, S.M. Yahaya, A. Ojo, T.O. Adaramoye, S.K. Ekundayo, A. Abdullahi, H. Badamasi. J. Nanopart. Res. **26**, *5*, 106 (2024). https://doi.org/10.1007/s11051-024-06006-2

[2] Yu.A. Baimova, R.R. Mulyukov. Grafen, nanotrubki i drugie uglerodnye nanostruktury. RAS, Moscow (2018). p. 212 (in Russian).

[3] W. Du, Z. Ahmed, Q. Wang, C. Yu, Z. Feng, G. Li, M. Zhang, C. Zhou, R. Senegor, C.Y. Yang. 2D Mater. **6**, *4*, 042005 (2019). https://doi.org/10.1088/2053-1583/ab41d3

[4] V.T. Dang, D.D. Nguyen, T.T. Cao, P.H. Le, D.L. Tran, N.M. Phan, V.C. Nguyen. Adv. Natur. Sci.: Nanosci. Nanotechnol. **7**, *3*, 033002 (2016). https://doi.org/10.1088/2043-6262/7/3/033002

[5] J. Sheng, Z. Han, G. Jia, S. Zhu, Y. Xu, X. Zhang, Y. Yao, Y. Li. Adv. Funct. Mater. **33**, *43*, 2306785 (2023). https://doi.org/10.1002/adfm.202306785

[6] A. Gbaguidi, S. Namilae, D. Kim. Nanotechnol. **31**, *25*, 255704 (2020). https://doi.org/10.1088/1361-6528/ab7fcc

[7] I.N. Kholmanov, C.W. Magnuson, R. Piner, J.Y. Kim, A.E. Aliev, C. Tan, T.Y. Kim, A.A. Zakhidov, G. Sberveglieri, R.H. Baughman, R.S. Ruoff. Adv. Mater. **27**, *19*, 3053 (2015). https://doi.org/10.1002/adma.201500785

[8] B. Liu, J. Sun, J. Zhao, X. Yun. Adv. Compos. Hybrid Mater. **8**, *1*, 1 (2025). https://doi.org/10.1007/s42114-024-01074-3

[9] S. Pyo, Y. Eun, J. Sim, K. Kim, J. Choi. Micro & Nano Syst. Lett. **10**, *1*, 9 (2022). https://doi.org/10.1186/s40486-022-00151-w

[10] S.C. Qin, Y. Liu, H. Jiang, Y. Xu, Y. Shi, R. Zhang, F. Wang. Sci. China Inf. Sci. **62**, *12*, 220403 (2019). https://doi.org/10.1007/s11432-019-2676-x

[11] X. Wu, F. Mu, H. Zhao. J. Mater. Sci. Technol. **55**, 16 (2020). https://doi.org/10.1016/j.jmst.2019.05.063

[12] B.Yu. Valeev, A.N. Toksumakov, D.G. Kvashnin, L.A. Chernozatonskii. JETP Lett. **115**, *2*, 93 (2022). https://doi.org/10.1134/S0021364022020114

[13] J. Srivastava, A. Gaur. J. Chem. Phys. **155**, *24*, 244104 (2021). https://doi.org/10.1063/5.0077099

[14] A.B. Felix, M. Pacheco, P. Orellana, A. Latgé. Nanomater. **12**, *19*, 3475 (2022). https://doi.org/10.3390/nano12193475

[15] Y. Gao, T. Cao, F. Cellini, C. Berger, W.A. de Heer, E. Tosatti, E. Riedo, A. Bongiorno. Nature Nanotechnol. **13**, *2*, 133 (2018). https://doi.org/10.1038/s41565-017-0023-9
[16] M. Elstner, D. Porezag, G. Jungnickel, J. Elsner, M. Haugk, Th. Frauenheim, S. Suhai, G. Seifert. Phys. Rev. B **58**, *11*, 7260 (1998). https://doi.org/10.1103/PhysRevB.58.7260
[17] B. Hourahine, B. Aradi, V. Blum, F. Bonafé, A. Buccheri, C. Camacho, C. Cevallos, M.Y. Deshaye, T. Dumitrică, A. Dominguez, S. Ehlert, M. Elstner, T. van der Heide, J. Hermann, S. Irle, J.J. Kranz, C. Köhler, T. Kowalczyk, T. Kubař, I.S. Lee, V. Lutsker, R.J. Maurer, S.K. Min, I. Mitchell, C. Negre, T.A. Niehaus, A.M.N. Niklasson, A.J. Page, A. Pecchia, G. Penazzi, M.P. Persson, J. Řezáč, C.G. Sánchez, M. Sternberg, M. Stöhr, F. Stuckenberg, A. Tkatchenko, V. W.-z. Yu, T. Frauenheim. J. Chem. Phys. **152**, *12*, 124101 (2020). https://doi.org/10.1063/1.5143190
[18] A.K. Rappe, C.J. Casewit, K.S. Colwell, W.A. Goddard III, W.M. Skiff. J. Am. Chem. Soc. **114**, *25*, 10024 (1992). https://doi.org/10.1021/ja00051a040
[19] S. Datta. Quantum Transport: Atom to Transistor. Cambridge University Press: Cambridge, London, UK (2005). 404 p.
[20] M. Li, X. Liu, X. Zhao, F. Yang, X. Wang, Y. Li. Top. Curr. Chem. (Z) **375**, *2*, 29 (2017). https://doi.org/10.1007/s41061-017-0116-9

Translated by A.Akhtyamov